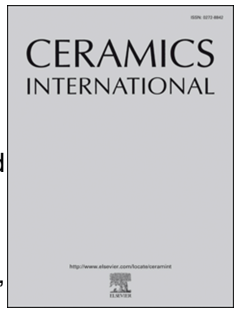

Crystal structure and thermomechanical properties of CaO-PSZ ceramics synthesised from fused ZrO_2

Guo Chen, Yeqing Ling, Qiannan Li, Hewen Zheng, Kangqiang Li, Qi Jiang, Jin Chen, Mamdouh Omran, Lei Gao

PII: S0272-8842(20)30700-8

DOI: https://doi.org/10.1016/j.ceramint.2020.03.079

Reference: CERI 24582

To appear in: *Ceramics International*

Received Date: 31 January 2020

Revised Date: 6 March 2020

Accepted Date: 7 March 2020

Please cite this article as: G. Chen, Y. Ling, Q. Li, H. Zheng, K. Li, Q. Jiang, J. Chen, M. Omran, L. Gao, Crystal structure and thermomechanical properties of CaO-PSZ ceramics synthesised from fused ZrO_2, *Ceramics International* (2020), doi: https://doi.org/10.1016/j.ceramint.2020.03.079.

Crystal structure and thermomechanical properties of CaO-PSZ ceramics synthesised from fused ZrO_2

Guo Chen [a, b], Yeqing Ling [a], Qiannan Li [a], Hewen Zheng [a], Kangqiang Li [b, 1], Qi Jiang [b], Jin Chen [a, b, *], Mamdouh Omran [c], Lei Gao [a, **]

[a] *Kunming Key Laboratory of Energy Materials Chemistry, Yunnan Minzu University, Kunming 650500, P.R. China.*

[b] *Faculty of Metallurgical and Energy Engineering, Kunming University of Science and Technology, Kunming 650093, P.R. China.*

[c] *Process Metallurgy Research Group, Faculty of Technology, University of Oulu, Finland.*

[*] Corresponding author: jinchen@kust.edu.cn

[**] Co-Corresponding author: glkust2013@hotmail.com

[1] The authors contributed equally to this work and should be regarded as co-first authors.

Abstract:

Partially stabilised zirconia (PSZ) ceramics have attracted much interest because of their outstanding properties. In this study, fused ZrO_2 was treated as a raw resource for the synthesis of CaO-PSZ ceramic materials through a facile sintering process. The crystal structure and thermomechanical properties of the synthesised CaO-PSZ ceramic samples were determined using XRD and SEM. The results revealed that various process parameters had different effects on the zirconia stability rate, including the temperature changing rate during the heating and cooling stages and the temperature and isothermal time during the quenching treatment; this was primarily a result of the thermodynamic characteristics of the martensitic conversion of ZrO_2 ceramics. Secondly, the martensitic conversion process was revealed by XRD patterns, expressed as the partial conversion of c-ZrO_2 to m-ZrO_2. Meanwhile, SEM-EDAX analysis highlighted the precipitation behaviour of the CaO stabiliser and the successful preparation of CaO-PSZ ceramics by sintering, represented by the gathering phenomenon of the acicular grains and particles, as the findings matched the stability rate analysis. This study can supply a sound reference for the synthesis of CaO-PSZ ceramics from fused ZrO_2.

Keywords: CaO-PSZ ceramics; fused ZrO_2; crystal structure; thermomechanical properties

1 Introduction

Zirconia (ZrO_2) materials have attracted increasing interest in the field of advanced ceramic materials because of their outstanding physical characteristics [1-4], such as high refractive index, high-temperature resistance, and low thermal conductivity [5-7]. However, a

large volume effect occurs during the heating and cooling processes for zirconia products, causing the accumulation of internal stress and the formation of defects, which can have a detrimental impact on the mechanical properties, seriously restricting the further applications of zirconia materials in many fields [8, 9].

Partially stabilised zirconia (PSZ) ceramic materials exhibit unparalleled physical performance, attributed to their unique martensitic transformation characteristics [10, 11]. Pure ZrO_2 materials maintain their form of m-ZrO_2 at room temperature, and two other phases exist in the high-temperature zone, called t-ZrO_2 and c-ZrO_2; furthermore, the three crystal phases can be converted among each other with changing temperature. Therefore, a reversible martensitic transformation occurs as the temperature increases or decreases. Specifically, as the temperature changes, the t-ZrO_2 phase will convert to the m-ZrO_2 phase at 1000 °C, and the transposed conversion for the m-ZrO_2 phase to the t-ZrO_2 phase arises at 1173 °C; the t-ZrO_2 phase will convert to the c-ZrO_2 phase with a transition temperature of 2370 °C [12, 13]. Garvie et al. showed that the acicular precipitation of the m-ZrO_2 phase in the cubic matrix had a significant strengthening effect on ceramic materials [14]. Thus, based on this finding, systematically applying the martensitic transformation characteristics of ZrO_2 materials to prepare PSZ ceramic materials can achieve a toughening effect for ZrO_2-based ceramic materials.

At present, PSZ ceramics are usually prepared by stabiliser doping. The stabilisers adopted include metal oxides whose cationic radius is close to that of the Zr^{4+} ion [15, 16], such as CaO [17, 18], MgO [19], CeO_2 [20], and Y_2O_3 [21]. Meanwhile, there are no significant differences between the crystal structures of those cations and that of the Zr^{4+} ion;

hence, those oxide cations can be used to replace the Zr^{4+} ion [22]. The essence of the toughening effect is the use of doping with oxides to introduce these cations into zirconia material whose radius is larger than the radius of Zr^{4+} ion, and these cations can substitute for the Zr^{4+} ion, further forming a stable replacement solid solution [23, 24]. In conclusion, producing PSZ ceramic materials with stabilised zirconia as the raw material can prevent the reduction of mechanical properties caused by the strong volume effect of monoclinic phase zirconia and retain the partial toughening effect of the martensitic transformation; therefore, it is the most suitable method for preparing structural materials and functional materials with zirconia as the matrix. Moreover, the introduction of microwave technology into the synthesis of PSZ ceramic materials leads to the increased performance of the ceramic products [25-30].

In the present work, fused ZrO_2 was utilised as a raw resource to manufacture CaO-PSZ ceramic materials through a facile sintering process; then, the crystal structure and thermomechanical properties of the synthesised CaO-PSZ ceramic samples and raw materials were determined by XRD and SEM-EDAX. Additionally, according to the obtained XRD patterns, the relationship between the process parameters and the stability rate of the CaO-PSZ ceramic samples was synthetically explored, including the temperature changing rate during the heating and cooling stages and the temperature and isothermal time during the quenching treatment.

2 Experimental

2.1 Materials

Fused ZrO_2 as a raw resource to manufacture CaO-PSZ ceramics was provided by an

industry in Yingkou City (Liaoning Province, P.R. China). The chemical analytical data for the fused ZrO_2 was provided by the manufacturer, detailed as follows: 95.1% ZrO_2, 3.8% CaO, 0.4% SiO_2, 0.3% Al_2O_3, 0.2% TiO_2, and 0.1% Fe_2O_3. The results revealed that the fused ZrO_2 sample was processed through stabiliser doping, using calcium oxide (CaO) as the stabiliser. Therefore, it could be speculated that the expected PSZ ceramic synthesised through the sintering process was also doped with CaO as the stabiliser, formally denoted CaO-PSZ ceramic.

2.2 Experimental procedure

A total of 50.0 g of fused zirconia raw material was sampled and then placed in a ceramic crucible with a diameter of 50 mm. Previous reports suggest that PSZ ceramics can be successfully synthesised at 1450 °C for 4 h utilising fused ZrO_2 as a raw resource [31]. The preparation of CaO-PSZ ceramics material processes as follows: fused ZrO_2 was first heated to a specific temperature and then held for a set duration time, followed by cooling the sample to another set temperature to be treated with a quenching process and isothermal treatment. Therefore, the sample inside of the ceramic crucible was heated to 1450 °C for 4 h in an electric resistance furnace (SGM3817B) with different heating rates, cooling rates, quenching temperatures, and isothermal treatment times. Wherein during the sintering preparation experiments of CaO-PSZ ceramic materials, the heating rate ranged from 1 °C/min, 4 °C/min, 7 °C/min and 10 °C/min, the cooling rate ranged from 1 °C/min, 2 °C/min, 4 °C/min, 6 °C/min, 8 °C/min, 10 °C/min, 20 °C/min, 40 °C/min and 400 °C/min, the quenching temperature ranged from 25 °C, 50 °C, 100 °C, 200 °C, 400 °C, 700 °C, 750 °C, 800 °C, 850 °C, 900 °C, 950 °C, 1000 °C, 1050 °C, 1100 °C, 1150 °C, 1200 °C, 1250 °C, 1300 °C,

1350 °C, 1400 °C and 1450 °C, the isothermal treatment time ranged from 0 h, 1 h, 2 h, 3 h, 4 h, 5 h. Once attaining the expected process conditions, the samples were systematically characterised to explore the relationships among the influencing factors and the crystal structure and thermomechanical properties of zirconia samples.

2.3 Characterisation

X-ray diffraction (D/Max 2500, Rigaku, Japan) was utilised to analyse the changes in the phase compositions of the synthesised CaO-PSZ ceramic samples and raw materials. Additionally, scanning electron microscopy (XL30ESEM-TMP, Philips, Holland) was used to determine the changes in the microstructure appearance of the zirconia samples. In addition, the elemental composition of zirconia samples after sintering was determined by EDAX characterisation.

3 Results and discussion

The stability rate represents the stability properties of zirconia ceramic materials, and the specific values of the stability rate can be determined based on the corresponding XRD characterisation patterns [32, 33]. Moreover, the synthesis of PSZ ceramics involves the following stages: the heating stage, the heat maintenance stage, the cooling stage, and the quenching stage. The stability rates and crystal structures of PSZ ceramics are affected by these process parameters. Consequently, in this work, the effects of these process parameters on the crystal structure and thermomechanical properties of the synthesised PSZ ceramic samples were comprehensively explored, including the temperature changing rate during the heating and cooling stages and the temperature and isothermal time during the quenching

treatment.

3.1 Characterisation by XRD

The influence of the process parameters during the sintering preparation experiments of CaO-PSZ ceramics materials on the phase structures of zirconia samples was comparatively explored with respect to the fused ZrO_2 raw resource and the synthesised PSZ ceramic samples. Wherein the XRD pattern of the fused ZrO_2 raw resource is depicted in Fig. 1, and the XRD patterns of the PSZ ceramics samples treated with different heating rates, cooling rates, quenching temperatures, and isothermal treatment times are depicted in Fig. 2 and Fig. 3.

As depicted in Fig. 1, only the c-ZrO_2 phase (JCPDS: 49-1642) was detected in the fused ZrO_2 raw resource; there is no m-ZrO_2 phase (JCPDS: 37-1484) or t-ZrO_2 phase (JCPDS: 42-1164), implying that the fused ZrO_2 raw resource can be classified as a PSZ ceramic material. Second, combining the analysis of the chemical composition and Fig. 1, the diffraction peak of the CaO component disappeared, indicating that the CaO stabiliser was perfectly dissolved in the raw resource, accompanied by the presence of the solid solution.

The relationship between the temperature changing rate during the heating stage and the crystal structure of the PSZ ceramic samples is depicted in Fig. 2(a). The PSZ ceramics were synthesised by maintaining the temperature at a maximum value of 1450 °C, with heating rates varying from 1 °C/min to 10 °C/min, a cooling rate of 4 °C/min, and a temperature of 950 °C and isothermal time of 4 h during the quenching treatment. As shown in Fig. 2(a), as the heating rate varied from 1 °C/min to 10 °C/min, there were no significant differences in the crystal compositions of the synthesised PSZ ceramic samples, reflecting the same phase

compositions consisting of mixed m-ZrO_2 phase and c-ZrO_2 phase. Meanwhile, the heating rate had an insignificant effect on the intensities of the zirconia diffraction peak; the peak intensities of the c-ZrO_2 phase at 29.92° and the m-ZrO_2 phase at 28.06° and 31.24° were absent of sharp changes. In contrast with the fused ZrO_2 raw resource, a new phase, the m-ZrO_2 phase, was detected in the synthesised PSZ ceramic samples; this phase transition is assigned to the martensitic conversion of ZrO_2 material. Specifically, with changing temperature, the t-ZrO_2 phase will convert to the m-ZrO_2 phase at 1000 °C, the transposed conversion for the m-ZrO_2 phase to the t-ZrO_2 phase arises at 1173 °C, and the t-ZrO_2 phase will convert to the c-ZrO_2 phase with a transition temperature of 2370 °C [32, 33]. The martensitic conversion of ZrO_2 material is primarily influenced by the crystal transformation temperature, and there was no obvious relationship with the temperature changing rate. The treatment temperature was maintained in the range of 950 °C to 1450 °C; thereby, the respective conversion of the t-ZrO_2 phase to the m-ZrO_2 phase and the c-ZrO_2 phase to the t-ZrO_2 phase arises, causing the formation of a new crystal phase, the c-ZrO_2 phase, generated through the martensitic conversion of ZrO_2 material.

The effects of the temperature changing rate during the cooling stage on the crystal structures of the synthesised ceramics samples are shown in Fig. 2(b). The PSZ ceramics were synthesised by maintaining the temperature at a maximum value of 1450 °C with a heating rate of 4 °C/min, a cooling rate varying from 1 °C/min to 400 °C/min, and a temperature of 950 °C and isothermal time of 4 h during the quenching treatment. As shown in Fig. 2(b), as the cooling rate varied from 1 °C/min to 4 °C/min, the diffraction peak intensity of the c-ZrO_2 phase was greatly enhanced and the peak intensities of the m-ZrO_2 phase also increased.

Furthermore, as the cooling rate increased to 400 °C/min, the peak intensities of the c-ZrO_2 phase still presented a substantial enhancement; however, the peak intensities of the m-ZrO_2 phase decreased. The difference between the two crystals suggests that the cooling rate had a significant relationship with the crystal transition of the synthesised PSZ ceramic samples, and the optimal value of the cooling rate could be determined to be in the range of 4 °C/min to 400 °C/min. Moreover, during the cooling process, the respective conversion process of the t-ZrO_2 phase to the m-ZrO_2 phase and the c-ZrO_2 phase to the t-ZrO_2 phase arises, and the increase in the cooling rate contributed to the completion degree of those conversion processes. Moreover, as the temperature decreased from 1450 °C to 1173 °C, a higher cooling rate was naturally accompanied by greater internal motion, further promoting the partial conversion process between the m-ZrO_2 phase and the t-ZrO_2 phase.

The influence of the temperature during the quenching treatment on the crystal structures of the synthesised PSZ ceramics samples is depicted in Fig. 2(c). The PSZ ceramics were synthesised by maintaining the temperature at a maximum value of 1450 °C with a heating rate of 4 °C/min, a cooling rate of 4 °C/min, and temperature varying from 1400 °C to 25 °C with an isothermal time of 4 h during the quenching treatment. As shown in Fig. 2(c), as the temperature during the quenching treatment decreased from 1450 °C to 950 °C, the diffraction peak intensity of c-ZrO_2 phase showed a dramatic decrease, but the peak intensities of the m-ZrO_2 phase gradually increased. In addition, with temperatures lower than 950 °C, there is no significant difference between the diffraction peak intensities of the two crystal phases in the synthesised PSZ ceramic samples, reflecting the same phase composition with mixed c-ZrO_2 phase and m-ZrO_2 phase. The change in the crystal structure with quenching

temperature was attributed to the conversion between the m-ZrO_2 phase and the t-ZrO_2 phase, which occurred at 1173 °C [32, 33]. As the temperature during the quenching treatment decreased, the respective conversion process of the t-ZrO_2 phase to the m-ZrO_2 phase and the c-ZrO_2 phase to the t-ZrO_2 phase continually proceeded, causing a decrease in the c-ZrO_2 phase component and the appearance of the m-ZrO_2 phase component in the synthesised PSZ ceramic samples, further demonstrating the phenomenon where the peak intensity of the m-ZrO_2 crystal increased and the peak intensities of the c-ZrO_2 crystal decreased.

The influence of the isothermal time during the quenching treatment on the crystal structures of the synthesised PSZ ceramic samples is depicted in Fig. 3. The PSZ ceramics were synthesised by maintaining the temperature at a maximum value of 1450 °C with a heating rate of 4 °C/min, cooling rate of 4 °C/min, the expected temperatures (1300 °C, 1100 °C, and 900 °C), and the isothermal time varying from 0 h to 5 h during the quenching treatment stage. As shown in Fig. 3(a), during the quenching treatment stage, at 1300 °C, there was no obvious relationship between the isothermal time and the crystal compositions of the synthesised PSZ ceramic samples, which is reflected in the fact that the diffraction peaks of the two crystals maintained their intensities. In addition, as concluded from Fig. 3(b)-(c), a similar phenomenon arose; in detail, when the temperature dropped to 1100 °C or 900 °C, there was no obvious relationship between the isothermal time and the crystal composition. Thus, the following conclusions can be obtained: during the quenching treatment stage, there was no obvious relationship between the isothermal time and the crystal structures of the synthesised PSZ ceramic samples.

3.2 Analysis of stability properties

The effects of the temperature changing rate during the heating and cooling stages and the temperature and isothermal time during the quenching treatment on the stability of the synthesised PSZ ceramic samples are plotted in Fig. 4; the results were calculated according to Eq. (1) and referring to the corresponding XRD patterns (depicted in Fig. 2 and Fig. 3).

$$\text{Stability rate} = \frac{\text{Intensity of } 29.92°}{\text{Intensity of } 28.06° + \text{Intensity of } 31.24° + \text{Intensity of } 29.92°} \times 100\% \quad (1)$$

Regarding the influence of the heating rate, as depicted in Fig. 4(a), the stability rate of the PSZ samples increased with increasing heating rate, with a slight increment, until it was basically in equilibrium. In detail, the stability rate was determined to be 74.3% at a heating rate of 1 °C/min, which slowly improved to 75.8% at 7 °C/min, and slightly decreased to 75.5% at 10 °C/min. Thus, the following conclusions can be obtained: during the heating stage, there was no obvious relationship between the heating rate and the stability properties of the synthesised PSZ ceramic samples. This finding can be attributed to the fact that the stability rate was determined using the XRD analysis patterns. Second, the martensitic conversion of ZrO_2 material is primarily related to the crystal transformation temperature; hence, there is no noticeable association with the temperature changing rate.

Regarding the influence of the temperature changing rate during the cooling process, as depicted in Fig. 4(b), the stability rate of the PSZ samples also increased with increasing cooling rate. In detail, the stability rate was determined to be 57.1% with a cooling rate of 1 °C/min, followed by an increase to 93.1% at a cooling rate of 20 °C/min; furthermore, once the cooling rate exceeded 20 °C/min, the increase in the stability rate was slight, as it was basically in equilibrium; the value of 93.1% at 20 °C/min slowly increased to 95.8% at

400 °C/min. This trend signified that the decrease in the cooling rate was favourable for the partial conversion of the t-ZrO_2 phase to the m-ZrO_2 phase. Thereby, to promote the synthesis of PSZ ceramics, the cooling rate should be maintained at a small value. As the cooling rate decreases, the stability rate of the PSZ ceramic samples will also decrease, indicating the more thorough formation of PSZ ceramic samples.

Regarding the influence of quenching treatment temperature, as shown in Fig. 4(c), as the quenching treatment temperature decreased, during the initial phase, the value of the stability rate of the PSZ ceramics samples tended to decrease gradually; meanwhile, the reduction of the stability rate value was much larger at the high-temperature stage, reflected by a value of 96.5% at 1450 °C that decreased to 75.2% at 950 °C. Moreover, when the quenching treatment temperature was much less than 950 °C, the increase in the stability rate value was slight, as it was basically in equilibrium; the value of 75.2% at 950 °C changed to 75.3% at 25 °C. This trend signified that the decrease in the quenching treatment temperature inhibited the partial conversion between the m-ZrO_2 phase and the t-ZrO_2 phase. Therefore, to promote the synthesis of PSZ ceramics, the quenching treatment temperature should be maintained at a high value during the cooling stage.

Regarding the influence of isothermal treatment time, as depicted in Fig. 4(d), at 1300 °C, the stability rate of the PSZ ceramic samples decreased from 89.3% to 88.1% as the isothermal treatment time varied from 0 h to 5 h; similarly, the stability rate decreased from 80.4% to 79.2% at 1100 °C, and it decreased from 74.9% to 73.5% at 900 °C. This trend with the isothermal treatment time was observed because in the cooling stage, once the quenching treatment temperature reached a certain low value, prolonging the isothermal treatment time

could not provide sufficient motivation for the partial conversion between the m-ZrO_2 phase and the t-ZrO_2 phase, further causing a slight variation in the stability rate.

3.3 SEM characterisation

The phase microstructures of the synthesised PSZ ceramic samples and fused ZrO_2 raw resource were determined by SEM characterisation; the corresponding images are shown in Fig. 5.

For the fused ZrO_2 raw resource, as displayed in Fig. 5(a)-(b), the sample consisted of overlapped scales, and there were no significant crystal defects, such as cracks or holes, indicating that the fused zirconia met the basic requirements for high-performance zirconia materials. As seen in Fig. 5(b), the crystal borders were distinct and regular. Moreover, in the magnified image shown in Fig. 5(c), the crystal border angles at the intersection points could be determined to be approximately 120°, signifying that the fused ZrO_2 raw resource consisted of the fluorite-structured c-ZrO_2 phase. This finding matched the XRD analysis results for the fused ZrO_2 raw resource (Fig. 1).

For the PSZ ceramic samples synthesised at 1450 °C for 4 h, as shown in Fig. 5(d)-(f), a more dense structure was observed to appear on the surface, without cracks, and agglomeration of the acicular grains and thin particles occurred (as depicted in Fig. 5(f)), indicating that the synthesised PSZ ceramic samples had a better structural performance than that of the fused ZrO_2 raw material. The agglomeration of the acicular grains and thin particles was caused by the CaO stabiliser deposited at the crystal borders. In addition, by comparison between Fig. 5(c) and Fig. 5(f), it is clear that the complete cubic-phase zirconia disappeared and was substituted by an iconic mixed-phase composition of PSZ ceramics,

revealing the successful synthesis of PSZ ceramic materials.

3.4 Characterisation by EDAX

The microscopic appearance and elemental semi-quantitative analysis of the PSZ ceramic sample synthesised at 1450 °C for 4 h are depicted in Fig. 6, wherein Fig. 6(a) shows the SEM image and Fig. 6(b), (c), and (d) shows the EDAX spectra of spot 1, spot 2, and spot 3, respectively.

As shown in Fig. 6(a), spot 1 is on the crystal boundary, whereas spot 2 and spot 3 are not. Thus, there existed a significant difference in the results of elemental semi-quantitative analysis at spot 1, spot 2, and spot 3. At spot 1, the elemental analysis revealed 15.37% CaO and 48.88% ZrO_2; 1.79% CaO and 78.68% ZrO_2 were determined at spot 2, and 4.66% CaO and 75.38% ZrO_2% were found at spot 3. Clearly, the content of CaO at spot 1 was much higher than that at spot 2 and spot 3; conversely, the ZrO_2 content at spot 1 was smaller.

Second, the precipitation of the CaO stabiliser at the crystal border was verified by the differences in the elemental composition distribution at the selected spots. At spot 2 and spot 3, whose locations were far away from the crystal border, the CaO content was much lower than that at spot 1. Additionally, the precipitation of the CaO stabiliser signified the successful synthesis of the CaO-PSZ ceramic materials. The findings summarised using the EDAX spectral analysis matched the SEM analysis results.

4 Conclusions

In this study, CaO-PSZ ceramic materials were efficiently synthesised using a facile sintering process, and the crystal structure and thermomechanical properties of the

synthesised CaO-PSZ ceramic samples were comprehensively investigated. The main findings can be summarised as follows:

(1) XRD patterns revealed that after sintering, the diffraction peak intensities of the c-ZrO_2 phase decreased and the diffraction peak intensities of the m-ZrO_2 phase increased, denoting the mixed phase structure of CaO-PSZ ceramics.

(2) The unique martensitic transformation of zirconia had a different influence on the stability rate of the synthesised CaO-PSZ ceramics among various process factors, as the stability rate increased with increasing temperature changing rate during the heating and cooling stages and the quenching treatment temperature, while there was no significant relationship with the isothermal time during the quenching treatment.

(3) SEM-EDAX analysis highlighted the precipitation behaviour of the CaO stabiliser and the successful sintering preparation of CaO-PSZ ceramics, represented by the agglomeration of the acicular grains and particles; these findings matched the stability rate analysis.

This work highlights the effective preparation of CaO-PSZ ceramic materials through conventional sintering of fused ZrO_2.

Acknowledgments

Financial support from the National Natural Science Foundation of China (Grant No. 51764052) and Innovative Research Team (in Science and Technology) at the University of Yunnan Province is gratefully acknowledged.

References

1. A. Rittidech, R. Somrit, T. Tunkasiri, Effect of adding Y_2O_3 on structural and mechanical properties of Al_2O_3-ZrO_2 ceramics, Ceram. Int. 39 (2013) 433-436. https://doi.org/10.1016/j.ceramint.2012.10.108.
2. L.A. Bicalho, C.A.R.P. Baptista, R.C. Souza, C. Santos, K. Strecker, M.J.R. Barboza, Fatigue and subcritical crack growth in ZrO_2-bioglass ceramics, Ceram. Int. 39(3) (2013) 2405-2414. https://doi.org/10.1016/j.ceramint.2012.08.093.
3. K.Q. Li, J. Chen, J.H. Peng, S. Koppala, M. Omran, G. Chen, One-step preparation of CaO-doped partially stabilized zirconia from fused Zirconia, Ceram. Int. 46(5) (2020) 6484-6490. https://doi.org/10.1016/j.ceramint.2019.11.129.
4. Z.Q. Guo, B.Q. Han, H. Dong, Effect of coal slag on the wear rate and microstructure of the ZrO_2-bearing chromia refractories, Ceram. Int. 23(6) (1997) 489-496. https://doi.org/10.1016/S0272-8842(96)00059-4.
5. D.K. Leung, C.J. Chan, M. Rühle, F.F. Lange, Metastable crystallization, phase partitioning, and grain growth of ZrO_2-Gd_2O_3 materials processed from liquid precursors, J. Am. Ceram. Soc. 74(11) (2005) 2786-2792. https://doi.org/10.1111/j.1151-2916.1991.tb06844.x.
6. C. Patapy, F. Gouraud, M. Huger, R. Guinebretière, B. Ouladiaff, D. Chateigner, T. Chotard, Investigation by neutron diffraction of texture induced by the cooling process of zirconia refractories, J. Eur. Ceram. Soc. 34(15) (2014) 4043-4052. https://doi.org/10.1016/j.jeurceramsoc.2014.05.027.
7. K.Q. Li, Q. Jiang, J. Chen, J.H. Peng, X.P. Li, S. Koppala, M. Omran, G. Chen, The controlled preparation and stability mechanism of partially stabilized zirconia by microwave intensification. Ceram. Int. 46(6) (2020) 7523-7530. https://doi.org/10.1016/j.ceramint.2019.11.251.

8. P.E. Reyes-Morel, I.W. Chen, Transformation plasticity of CeO_2-stabilized tetragonal zirconia polycrystals: I, stress assistance and autocatalysis, J. Am. Ceram. Soc. 71(5) (2010) 343-353. https://doi.org/10.1111/j.1151-2916.1988.tb05052.x.

9. L.L. Fehrenbacher, L.A. Jacobson, Metallographic observation of the monoclinic-tetragonal phase transformation in ZrO_2, J. Am. Ceram. Soc. 2010, 48(3) (2010) 157-161. https://doi.org/10.1111/j.1151-2916.1965.tb16054.x.

10. M.J. Readey, A.H. Heuer, R.W. Steinbrech, Annealing of test specimens of high□ toughness magnesia□partially□stabilized zirconia, J. Am. Ceram. Soc. 71(1) (2010) 2-6. https://doi.org/10.1111/j.1151-2916.1988.tb05766.x.

11. S. Guo, Y. Kagawa, Isothermal and cycle properties of EB-PVD yttria-partially-stabilized zirconia thermal barrier coatings at 1150 and 1300 °C, Ceram. Int. 33(3) (2007) 373-378. https://doi.org/10.1016/j.ceramint.2005.10.005.

12. M.H. Bocanegra-Bernal, S.D. De La Torre, Phase transitions in zirconium dioxide and related materials for high performance engineering ceramics, J. Mater. Sci. 37(23) (2002) 4947-4971. https://doi.org/10.1023/a:1021099308957.

13. R.H.J. Hannink, P.M. Kelly, B.C. Muddle, Transformati on toughening in zirconia-containing ceramics, J. Am. Ceram. Soc. 83(3) (2002) 461-487. https://doi.org/10.1111/j.1151-2916.2000.tb01221.x.

14. R.G. Garvie, R.H. Hannink, R.T. Pascoe, Ceramic steel, Nature. 258 (1975) 703-704. https://doi.org/10.1038/258703a0.

15. L. Hao, J. Lawrence, G.C. Lim, H.Y. Zheng, Examination of CO_2 laser-induced rapid solidification structures on magnesia partially stabilised zirconia and the effects thereof on wettability characteristics, Opt. Lasers. Eng. 42(3) (2004) 355-374. https://doi.org/10.1016/j.optlaseng.2003.10.002.

16. L. Hao, J. Lawrence, D.K.Y. Lowb, G.C. Limb, H.Y. Zheng, Correlation of the hydroxyl bond and wettability characteristics of a magnesia partially stabilised zirconia following CO_2 laser irradiation, Thin. Solid. Films. 468(1-2) (2004) 12-16. https://doi.org/10.1016/j.tsf.2004.03.032.

17. R.C. Garvie, G.H.J. Hannink, C. Urbani, Fracture mechanics study of a transformation toughened zirconia alloy in the CaO-ZrO_2 system, Ceram. Int. 6(1) (1985) 19-24. https://doi.org/ 10.1016/0390-5519(80)90028-9.

18. R.C. Garvie, Structure and thermomechanical properties of partially stabilized zirconia in the CaO-ZrO_2 system, J. Am. Ceram. Soc. 55 (2010) 152-157. https://doi.org/10.1007/978-94-009-0741-6_15.

19. M.J. Readey, R.R. Lee, J.W. Halloran, A. Heueret, Processing and sintering of ultrafine MgO-ZrO_2 and (MgO, Y_2O_3) -ZrO_2 powders, J. Am. Ceram. Soc. 73(6) (2010) 1499-1503. https://doi.org/10.1111/j.1151-2916.1990.tb09786.x.

20. E. Tani, M. Yoshimura, S. Somiya, Revised phase diagram of the system ZrO_2-CeO_2 below 1400 °C, J. Am. Ceram. Soc. 66(7) (2010) 506-510. https://doi.org/10.1111/j.1151-2916.1983.tb10591.x.

21. K. Chihwei, Y. Shen, F. Yen, H. Cheng, I. Hung, S. Wen, M. Wang, M. Stack, Phase transformation behavior of 3mol% yttria partially-stabilized ZrO_2 (3Y-PSZ) precursor powder by an isothermal method, Ceram. Int. 40 (2014) 3243-3251. https://doi.org/10.1016/j.ceramint.2013.09.112.

22. A. Bogicevic, C. Wolverton, G.M. Crosbie, E.B. Stechel, Defect ordering in aliovalently doped cubic zirconia from first principles. Phys. Rev. B. 64(1) (2001) 014106. https://doi.org/10.1103/PhysRevB.64.014106.

23. H. Wang, M.H. Wang, W.Y. Zhang, N. Zhao, W. Wei, Y.H. Sun, Synthesis of dimethyl carbonate from propylene carbonate and methanol using CaO-ZrO_2 solid solutions as

highly stable catalysts, Catal. Today. 115(1) (2006) 107-110. https://doi.org/10.1016/j.cattod.2006.02.031.

24. H. Wang. M.H Wang, N. Zhao, W. Wei, Y. Sun, CaO-ZrO_2 solid solution: a highly stable catalyst for the synthesis of dimethyl carbonate from propylene carbonate and methanol, Catal. Lett. 105(3-4) (2005) 253-257. https://doi.org/10.1007/s10562-005-8699-0.
25. K.Q. Li, J. Chen, G. Chen, J.H. Peng, R. Ruan, C. Srinivasakannan, Microwave dielectric properties and thermochemical characteristics of the mixtures of walnut shell and manganese ore, Bioresource. Technol. 286 (2019) 121381. https://doi.org/10.1016/j.biortech.2019.121381.
26. G. Chen, Q. Jiang, K.Q. Li, A.X. He, J.H. Peng, M. Omran, J. Chen, Simultaneous removal of Cr(III) and V(V) and enhanced synthesis of high-grade rutile TiO_2 based on sodium carbonate decomposition, J. Hazard. Mater. 388 (2020) 122039. https://doi.org/10.1016/j.jhazmat.2020.122039.
27. K.Q. Li, G. Chen, J. Chen, J.H. Peng, R. Ruan, C. Srinivasakannan, Microwave pyrolysis of walnut shell for reduction process of low-grade pyrolusite, Bioresource. Technol. 291 (2019) 121838. https://doi.org/10.1016/j.biortech.2019.121838.
28. K.Q. Li, J. Chen, J.H. Peng, R. Ruan, M. Orman, G. Chen, Dielectric properties and thermal behavior of electrolytic manganese anode mud in microwave field, J. Hazard. Mater. 381 (2020) 121227. https://doi.org/10.1016/j.jhazmat.2019.121227.
29. K.Q. Li, G. Chen, X.T. Li, J.H. Peng, R. Ruan, M. Omran, J. Chen, High-temperature dielectric properties and pyrolysis reduction characteristics of different biomass-pyrolusite mixtures in microwave field, Bioresource. Technol. 294 (2019) 122217. https://doi.org/10.1016/j.biortech.2019.122217.

30. K.Q. Li, J. Chen, J.H. Peng, R. Ruan, C. Srinivasakannan, G. Chen, Pilot-scale study on enhanced carbothermal reduction of low-grade pyrolusite using microwave heating, Powder. Technol. 360 (2020) 846-854. https://doi.org/10.1016/j.powtec.2019.11.015.

31. S.H. Guo, G. Chen, J.H. Peng, J. Chen, J.L. Mao, D.B. Li, L.J. Liu, Preparation of partially stabilized zirconia from fused zirconia using sintering, J. Alloy. Compd. 506 (1) (2010) L5-L7. https://doi.org/10.1016/j.jallcom.2010.06.156.

32. Y. Murase, E. Kato, K. Daimon, Stability of ZrO_2 phases in ultrafine ZrO_2-Al_2O_3 mixtures, J. Am. Ceram. Soc. 69(2) (1986) 83-87. https://doi.org/10.1111/j.1151-2916.1986.tb04706.x.

33. M.Y. Zhang, L. Gao, J.X. Kang, J. Pu, J.H. Peng, M. Omran, G. Chen, Stability optimisation of CaO-doped partially stabilised zirconia by microwave sintering, Ceram. Int. 45(17) (2019) 23278-23282. https://doi.org/10.1016/j.ceramint.2019.08.024.

Figure captions

Fig. 1 XRD pattern of fused zirconia raw material.

Fig. 2 XRD patterns of zirconia material treated with (a) different heating rates; (b) different cooling rates; (c) different quenching temperatures.

Fig. 3 XRD patterns of zirconia material treated with different isothermal treatment times, (a) 1300 °C; (b) 1100 °C; (c) 900 °C.

Fig. 4 Effects of process parameters on zirconia stability rate, (a) heating rate; (b) cooling rate; (c) quenching temperature; (d) isothermal treatment time.

Fig. 5 SEM images of zirconia material before and after sintering, (a) raw material, 50×; (b) 200×; (c) 1000×; (d) sintered sample, 500×; (e) 2000×; (f) 2000×.

Fig. 6 SEM image and EDAX spectra of zirconia material sintered at 1450 °C for 4 h, (a) SEM image; (b) EDAX of spot 1; (c) EDAX of spot 2; (d) EDAX of spot 3.

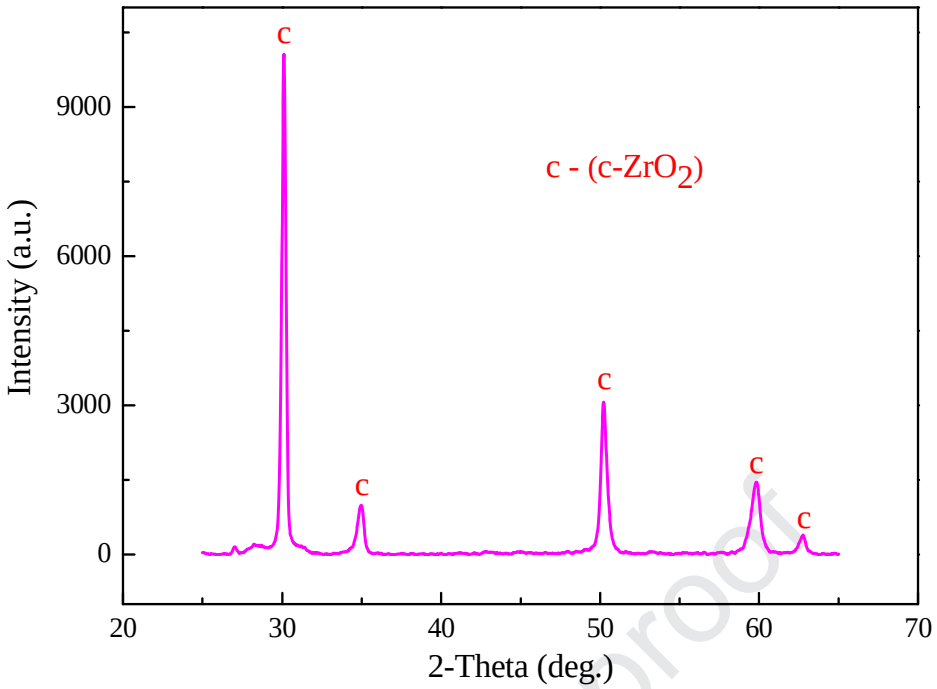

Fig. 1 XRD pattern of fused zirconia raw material.

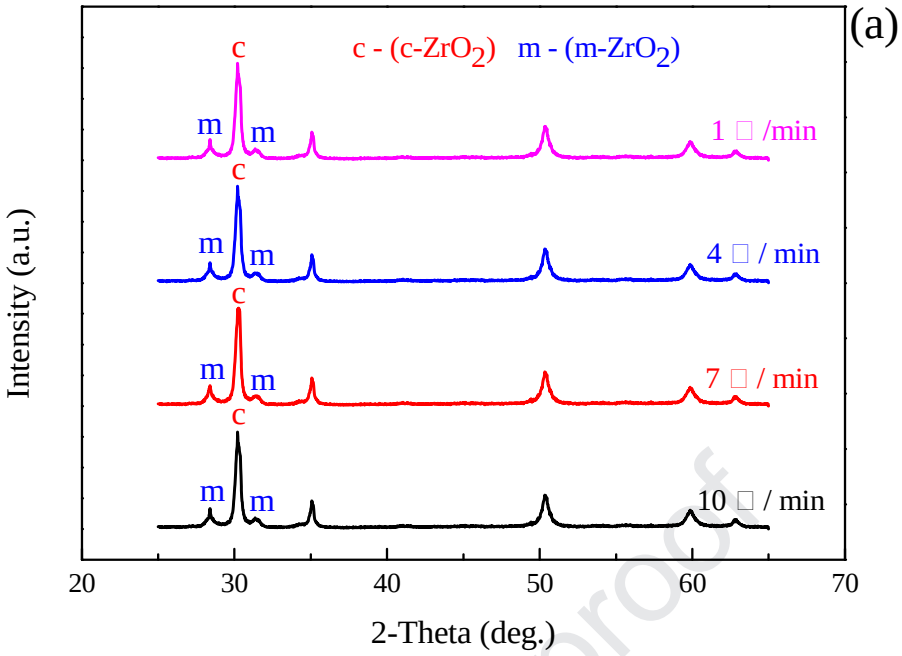

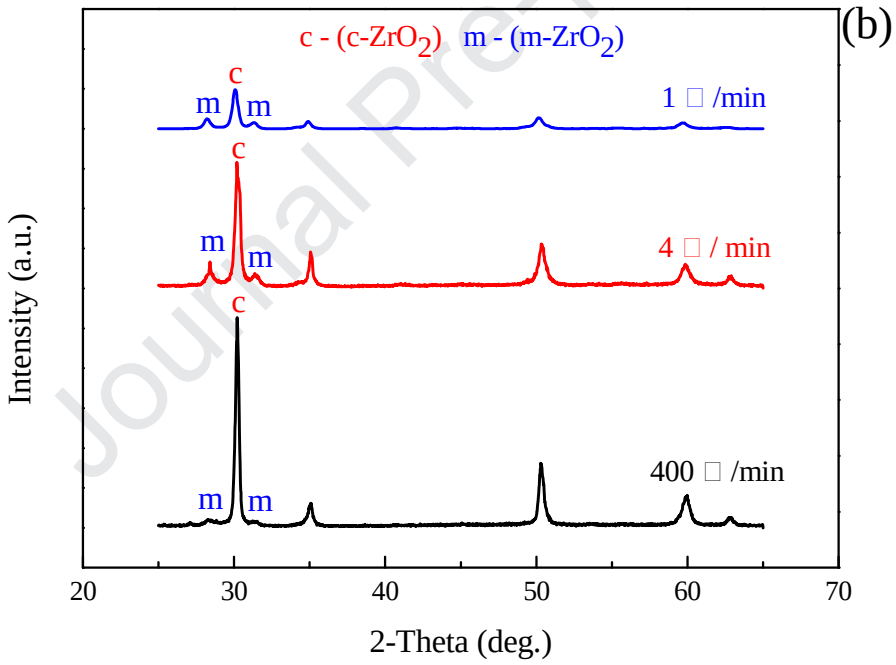

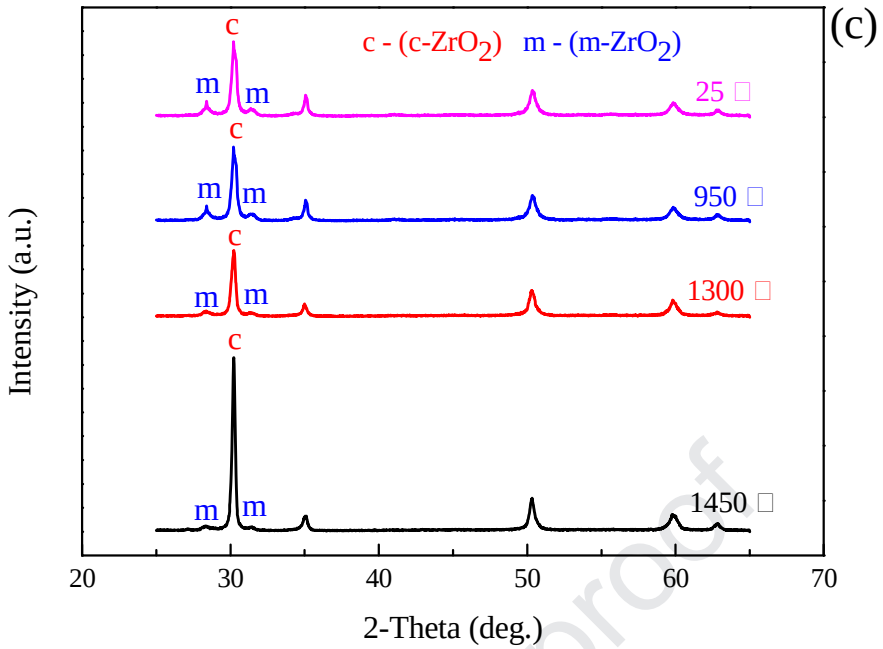

Fig. 2 XRD patterns of zirconia material treated with (a) different heating rates; (b) different cooling rates; and (c) different quenching temperatures.

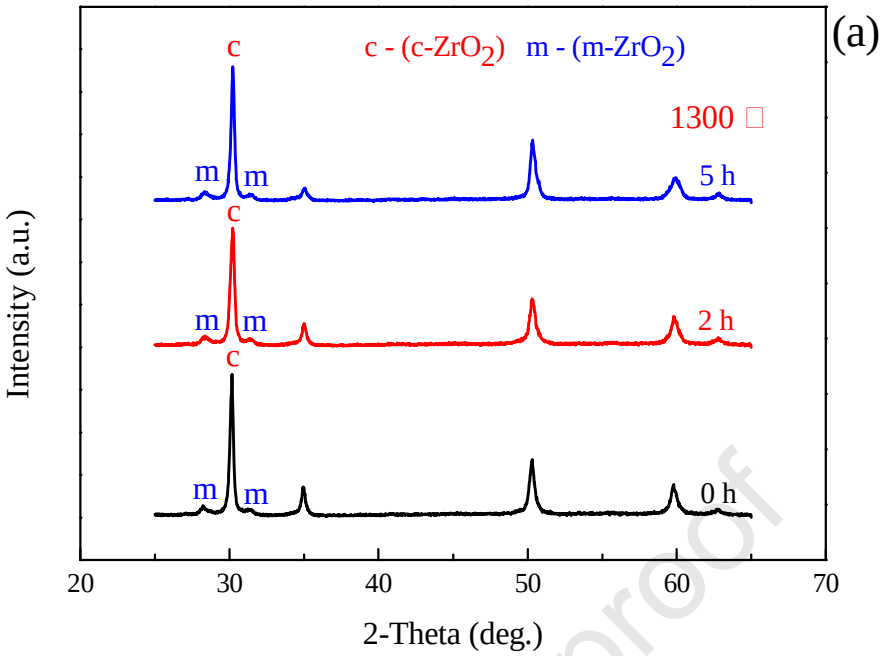

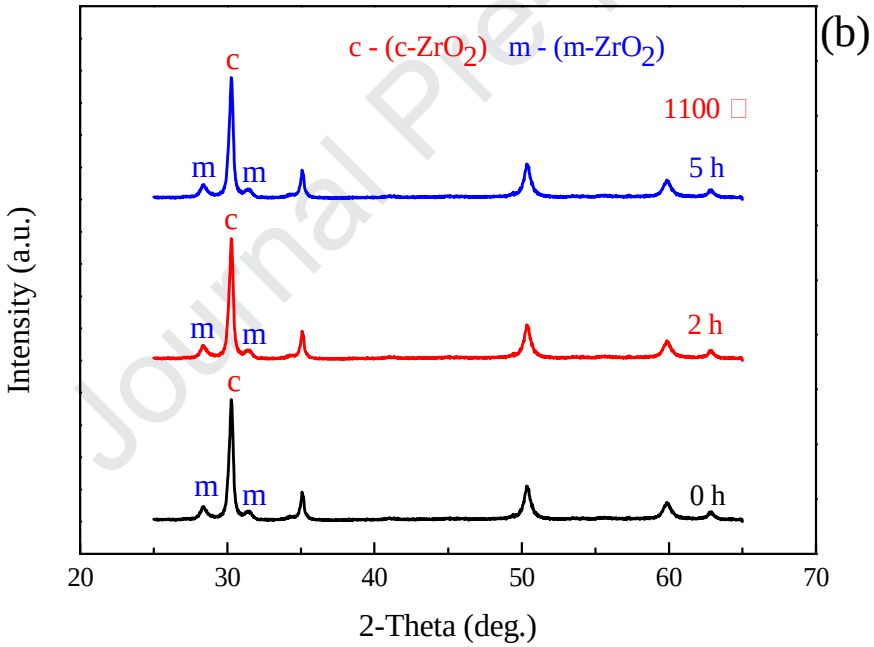

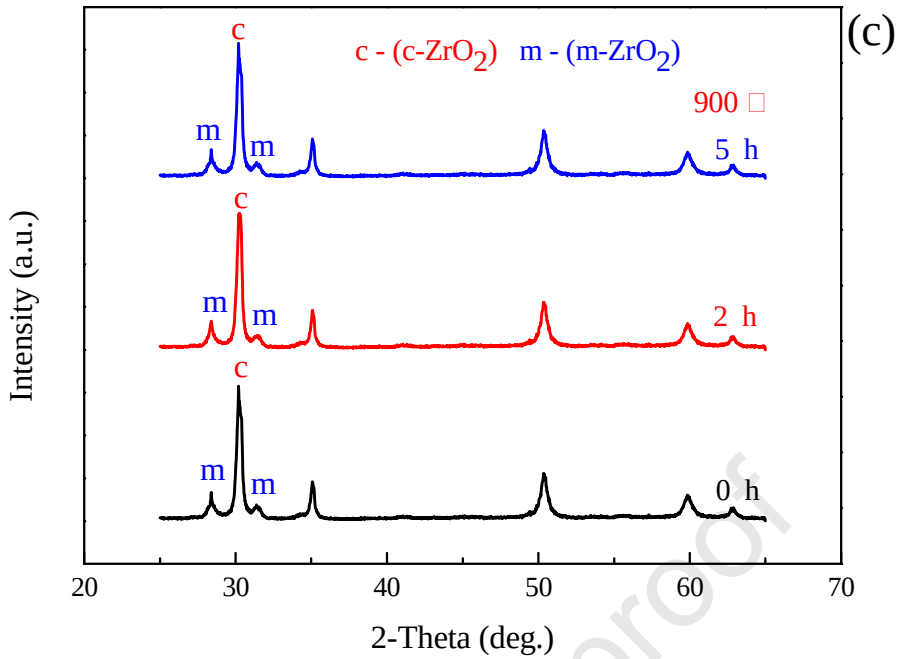

Fig. 3 XRD patterns of zirconia material treated with different isothermal treatment times, (a) 1300 °C; (b) 1100 °C; (c) 900 °C.

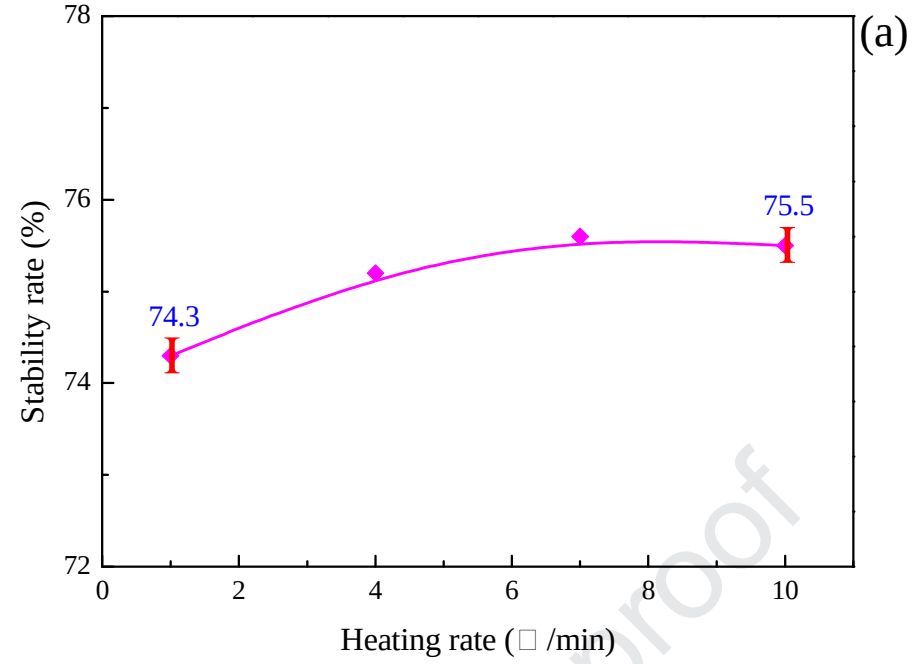

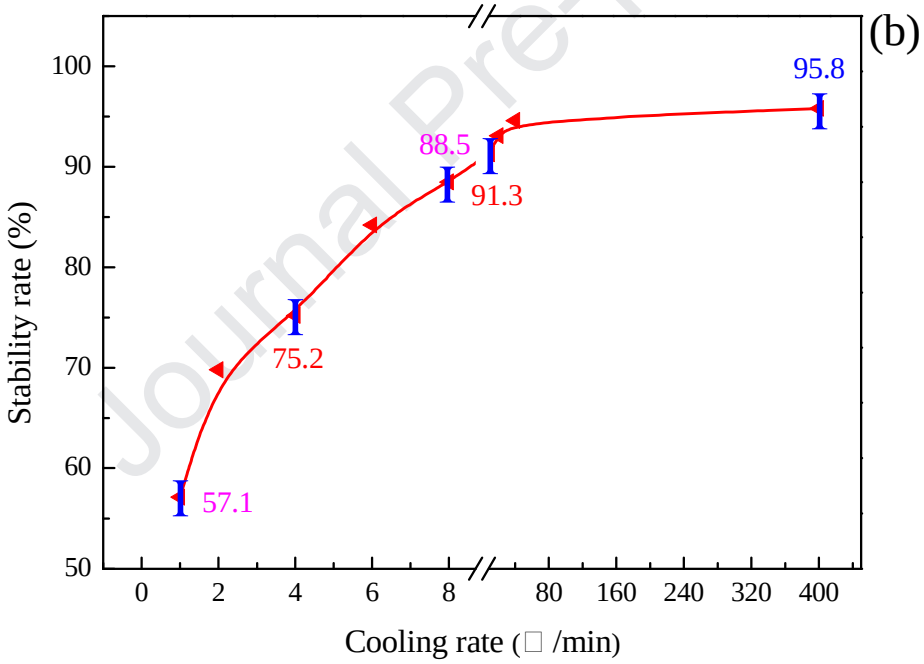

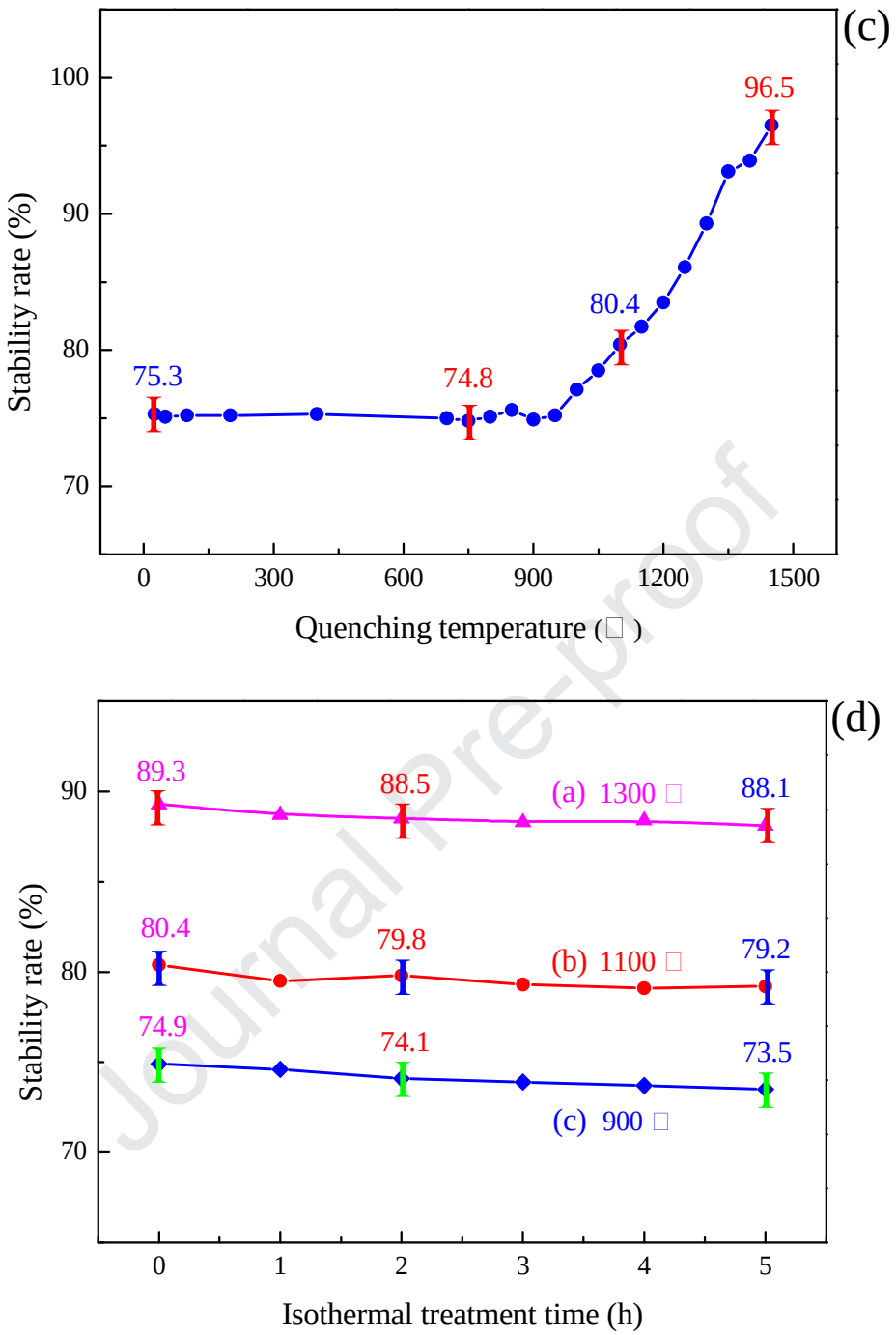

Fig. 4 Effects of process parameters on zirconia stability rate, (a) heating rate; (b) cooling rate; (c) quenching temperature; (d) isothermal treatment time.

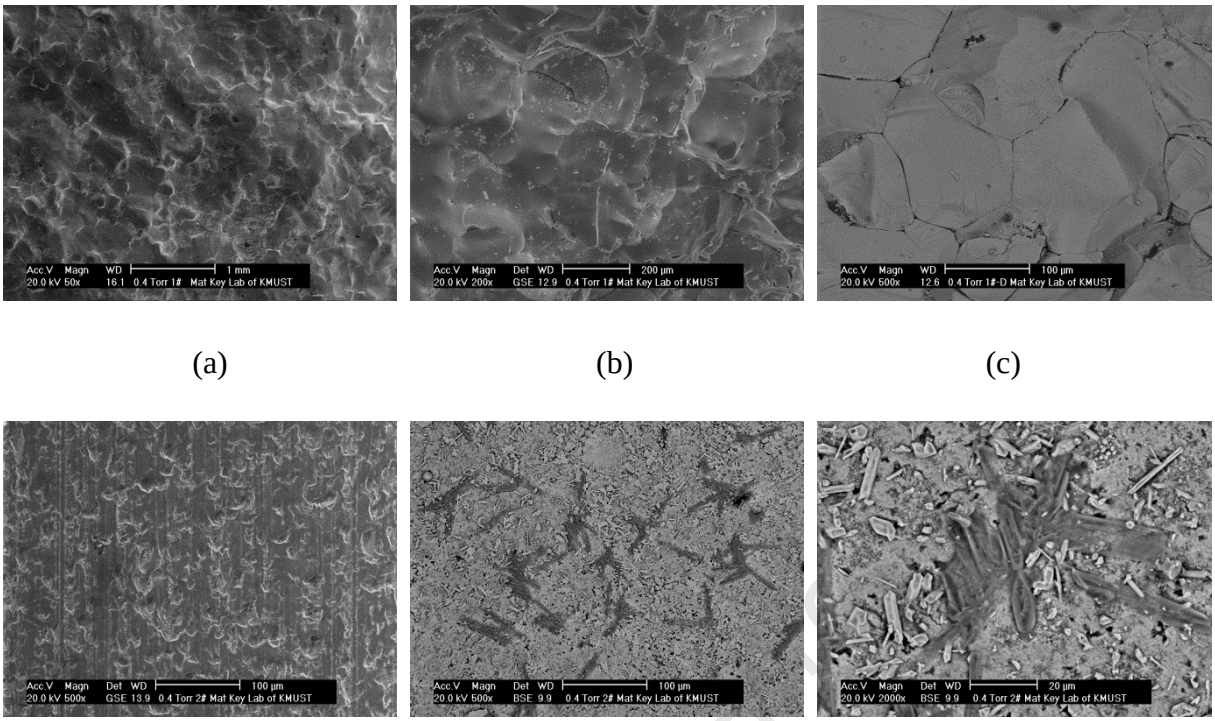

Fig. 5 SEM images of zirconia material before and after sintering, (a) raw material, 50×; (b) 200×; (c) 1000×; (d) sintered sample, 500×; (e) 2000×; (f) 2000×.

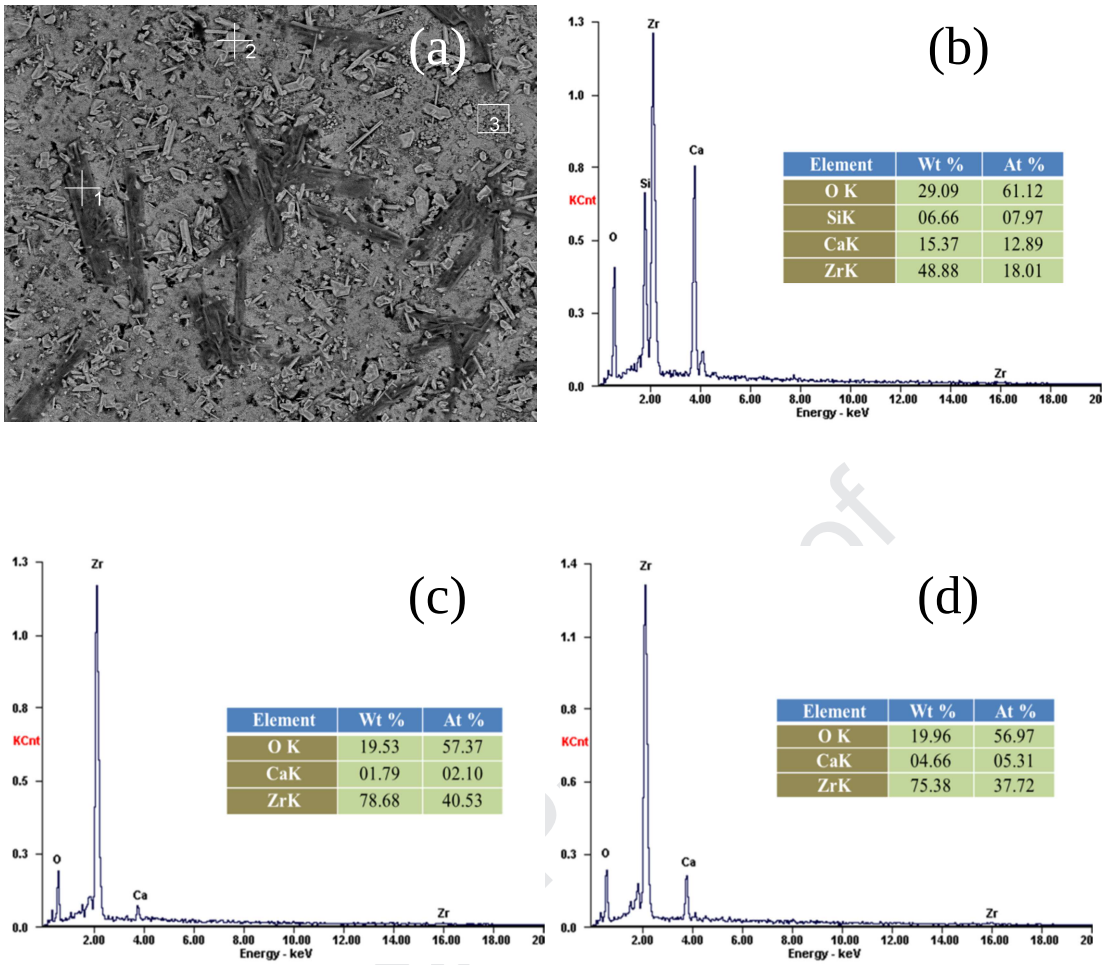

Fig. 6 SEM image and EDAX spectra of zirconia material sintered at 1450 °C for 4 h, (a) SEM image; (b) EDAX of spot 1; (c) EDAX of spot 2; (d) EDAX of spot 3.

Declaration of interests

☒ The authors declare that they have no known competing financial interests or personal relationships that could have appeared to influence the work reported in this paper.

☐The authors declare the following financial interests/personal relationships which may be considered as potential competing interests: